BIOCHEMISTRY
including biophysical chemistry & molecular biology

Article

pubs.acs.org/biochemistry

Increased Turnover at Limiting O_2 Concentrations by the Thr^{387} → Ala Variant of HIF-Prolyl Hydroxylase PHD2

Serap Pektas, Cornelius Y. Taabazuing, and Michael J. Knapp*

Department of Chemistry, University of Massachusetts, Amherst, Massachusetts 01003, United States

Supporting Information

ABSTRACT: PHD2 is a 2-oxoglutarate, non-heme Fe^{2+}-dependent oxygenase that senses O_2 levels in human cells by hydroxylating two prolyl residues in the oxygen-dependent degradation domain (ODD) of HIF1α. Identifying the active site contacts that determine the rate of reaction at limiting O_2 concentrations is crucial for understanding how this enzyme senses pO_2 and may suggest methods for chemically altering hypoxia responses. A hydrogen bonding network extends from the Fe(II) cofactor through ordered waters to the Thr^{387} residue in the second coordination sphere. Here we tested the impact of the side chain of Thr^{387} on the reactivity of PHD2 toward O_2 through a combination of point mutagenesis, steady state kinetic experiments and $\{FeNO\}^7$ EPR spectroscopy. The steady state kinetic parameters for Thr^{387} → Asn were very similar to those of wild-type (WT) PHD2, but k_{cat} and $k_{cat}/K_{M(O_2)}$ for Thr^{387} → Ala were increased by roughly 15-fold. X-Band electron paramagnetic resonance spectroscopy of the $\{FeNO\}^7$ centers of the (Fe+NO+2OG) enzyme forms showed the presence of a more rhombic line shape in Thr^{387} → Ala than in WT PHD2, indicating an altered conformation for bound gas in this variant. Here we show that the side chain of residue Thr^{387} plays a significant role in determining the rate of turnover by PHD2 at low O_2 concentrations.

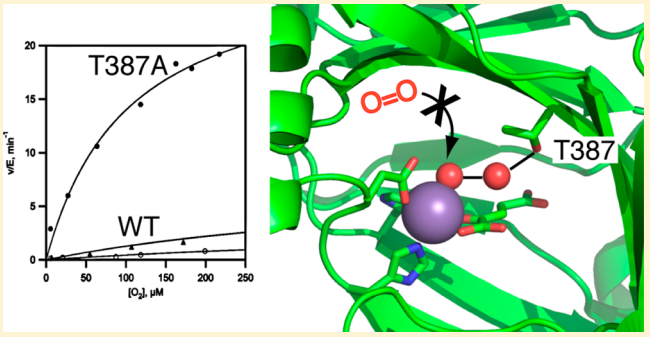

HIF prolyl-4-hydroxylase 2 (PHD2) is a non-heme Fe(II), 2-oxoglutarate (2OG)-dependent oxygenase that serves as the primary O_2 sensor in human cells.[1,2] PHD2 regulates the transcriptional activity of the hypoxia-inducible factor-1α (HIF-1α) transcription factor by hydroxylating Pro^{402} and Pro^{564} within the oxygen-dependent degradation domain (ODD) of HIF-1α.[1,3−5] As HIF-1α hydroxylation underlies angiogenesis and the balance between aerobic and anaerobic metabolism, PHD2 plays a crucial role in health conditions such as ischemia, anemia, and cancer.[6,7] Identifying the structural features of PHD2 that determine the reaction rate under conditions of limiting O_2 concentrations could point the way to altering cellular hypoxia sensing.

The (Fe+2OG)PHD2 form of the enzyme contains an Fe(II) cofactor coordinated by a His_2Asp facial triad, a bidentate 2OG ligand, and an aquo ligand. PHD2 is thought to follow the consensus chemical mechanism for 2OG oxygenases (Scheme 1).[8−10] When substrate ODD binds near the cofactor, the aquo ligand is released in analogy to other 2OG oxygenases, permitting O_2 to bind at the Fe for subsequent chemistry. Oxidative decarboxylation generates the ferryl $(FeO)^{2+}$, an intermediate that has been observed in related enzymes,[8,9,11,12] which hydroxylates the Pro target residue to complete the chemical steps of turnover (Scheme 1). Notably, PHD2 appears to be rate-limited by a step associated with O_2 binding or oxidative decarboxylation, as the $(FeO)^{2+}$ intermediate did not accumulate in the presteady state for PHD2,[10] and PHD2 exhibited an inverse solvent kinetic isotope effect (KSIE).[13,14] This is in contrast to other 2OG oxygenases in which the $(FeO)^{2+}$ accumulates in the presteady state, for which product release or hydroxylation appears to be the rate-limiting step.[8,9,11,12]

The connection between substrate binding and O_2 activation is crucial to understanding the chemistry of this class of enzyme. A recent study revealed a conserved pattern of second-sphere contacts in enzymes structurally related to PHD2[15] that may be functionally significant. The X-ray crystal structure of (Fe+2OG)PHD2[16] showed a hydrogen bonding network connecting the aquo ligand and 2OG to the side chain of Thr^{387} (Figure 1). Thr^{387} is located on the second β-strand, at a position that forms a conserved H-bond in many 2OG oxygenases.[15] As O_2 activation is integral to the function of PHD2 and other 2OG oxygenases, the disposition of Thr^{387} may be crucial to gas binding and reactivity.

Here we tested the role of second-sphere contacts from Thr^{387} on PHD2 hydroxylation chemistry through steady state kinetics and $\{FeNO\}^7$ EPR spectroscopy. Steady state kinetic parameters for the Thr^{387} → Asn variant, which conserved the hydrogen bonding capacity at this position, were very similar to those of wild-type (WT) PHD2. Remarkably, the macroscopic

Received: December 18, 2014
Revised: April 6, 2015
Published: April 10, 2015

DOI: 10.1021/bi501540c
Biochemistry 2015, 54, 2851−2857

Scheme 1. Consensus Chemical Mechanism for PHD2

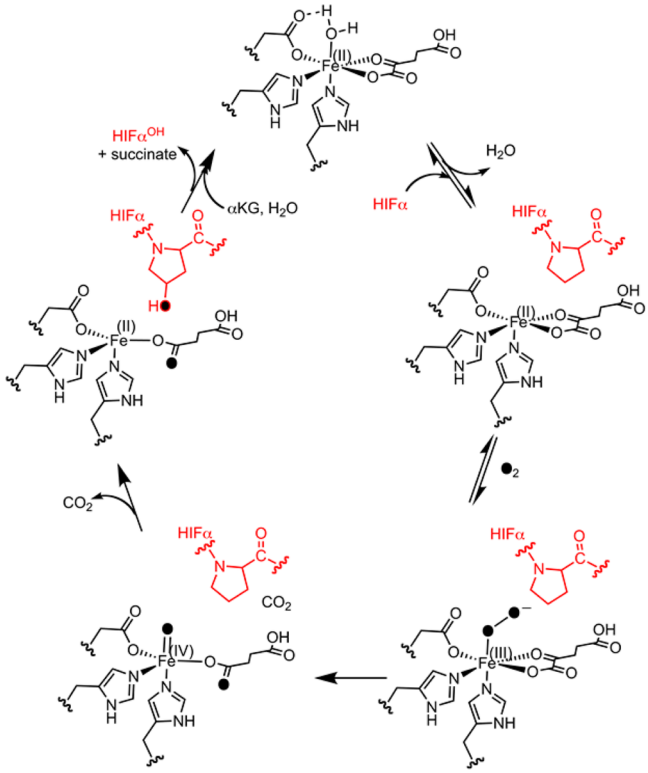

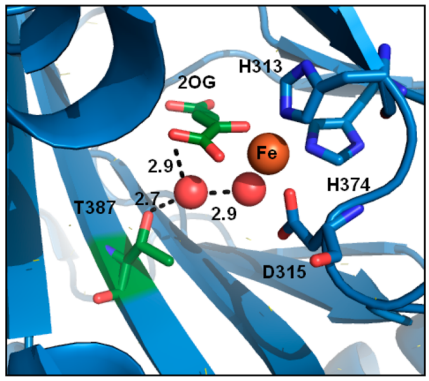

Figure 1. PHD2 active site (Protein Data Bank entry 3OUJ).[16] Waters are shown as red spheres, and distances are in angstroms.

rate constants for the Thr^{387} → Ala variant were 15 times larger than for WT PHD2, which is attributed to faster O_2 activation. Substrate inhibition was observed for the Thr^{387} → Ala variant, which implicates product release as a slow step in this variant—a corollary is that other substrate inhibition in other 2OG oxygenases likely reflects slow succinate release.[17] These results suggest that the second-sphere contacts from Thr^{387} slow turnover such that decarboxylation chemistry is rate-limiting in WT PHD2.

MATERIALS AND METHODS

Materials. All chemicals were purchased from commercial vendors and used without purification. The sequences of the peptide substrates were derived from the native HIF-1$\alpha^{556-574}$ (CODD) sequence. The sequence of the CODD peptide was DLDLEALAP^{564}YIPADDDFQL. The underlined residues were changed from the native sequences as follows: CODD (M561A, M568A) to avoid methionine oxidation. The CODD peptide (99% pure) was purchased from GL Biochem LTD (Shanghai, China).

Protein Expression and Purification. Recombinant human PHD2$_{178-426}$ and its variants, Thr^{387} → Ala and Thr^{387} → Asn, were expressed as C-terminal GST fusion proteins from *Escherichia coli* BL21(DE3) cells using a pGEX-4T-1 vector (Stratagene) and purified as previously described.[14,18] Briefly, PHD2-GST was purified using an affinity column (GSTrap, GE Bioscience), and then the GST tag was cleaved with restriction grade thrombin for 16 h at 4 °C. The thrombin was removed with a Hitrap Benzamidine column (GE Bioscience), and then PHD2 was treated with 50 mM EDTA overnight to remove metals. PHD2 was buffer exchanged with 50 mM HEPES (pH 7.50) and stored at −20 °C. The masses of WT PHD2 and the variants were determined by a QStar-XL hybrid quadrupole-TOF mass spectrometer (Applied Biosystems): WT PHD2 (27786.6 Da calculated, 27784.7 Da observed), Thr^{387} → Ala (27755.2 Da calculated, 27756.2 Da observed), and Thr^{387} → Asn (27799.6 Da calculated, 27798.2 Da observed).

Steady State Kinetic Assays. Steady state kinetic constants obtained from initial rates were measured at saturating concentrations of $(NH_4)_2Fe(SO_4)_2$ (10 μM) and ascorbic acid (1 mM) in 50 mM HEPES buffer (pH 7.00) at 37.0 °C. MALDI-TOF was used to measure the production of hydroxylated product CODD^{OH} [(M + O + Na$^+$), m/z 2174 calculated, m/z 2172 observed] from the substrate peptide CODD [(M + Na$^+$), m/z 2158 calculated, m/z 2156 observed]. Substrate inhibition constants were obtained by fitting the initial rate data to eq 1, in which the initial rate (v_0) is a function of the maximal rate (v_{max}), the Michaelis constant (K_M) and the inhibition constant (K_i) for the substrate (S).

$$v_0 = \frac{V_{max}}{1 + \frac{K_M}{[S]} + \frac{[S]}{K_i}} \quad (1)$$

For assays in which the 2OG concentration was varied, the concentration of CODD (10 μM) was fixed at saturating levels. Reactions were quenched at different time points in saturated 4-α-cyanohydroxycinnamic acid dissolved in 75% acetonitrile and 0.2% trifluoroacetic acid. Quenched reactions were spotted onto a MALDI target plate and analyzed using a Bruker Daltonics Omniflex MALDI-TOF mass spectrometer. For assays in which the CODD concentration varied, the concentration of 2OG (100 μM) was fixed at saturating.

Assays in which O_2 was the varied substrate used saturating concentrations of $(NH_4)_2Fe(SO_4)_2$ (10 μM), 2OG (100 μM), CODD (10 μM), and ascorbic acid (1 mM) in 50 mM HEPES (pH 7.00) at 37.0 °C. The concentration of dissolved O_2 was controlled by varying the ratio of N_2 and O_2 gas flowing through separate flow meters through a gas washer into an Atmosbag (Sigma-Aldrich), with the dissolved O_2 concentration monitored with a YSI model 5300 biological oxygen monitor. Reactions were quenched and analyzed as described for other steady state reactions.

2OG Binding. The dissociation constant (K_D) of 2OG was determined by measuring the quenching of the intrinsic tryptophan fluorescence of PHD2 upon binding 2OG. Samples were excited at 295 nm, and the emission was measured at 330 nm using a PTI spectrofluorometer (PTI-QM-4 2005SE). A cuvette containing PHD2 (1 μM) and $MnSO_4$ (20 μM) in 50 mM HEPES (pH 7.00) was titrated with aliquots of 2OG (500

DOI: 10.1021/bi501540c
Biochemistry 2015, 54, 2851−2857

Table 1. Steady State Kinetics of WT PHD2 and Variants with Varied 2OG Concentrations[a]

enzyme	k_{cat} (min^{-1})	$k_{cat}/K_{M(2OG)}$ (μM^{-1} min^{-1})	$K_{I(2OG)}$ (μM)	$K_{M(2OG)}$ (μM)	$K_{D(2OG)}$[b] (μM)
WT PHD2	2.3 ± 0.1	2.7 ± 0.4	$>2.6 \times 10^4$	0.9 ± 0.2	0.7 ± 0.2
Thr^{387} → Ala	32.9 ± 1.4	2.7 ± 0.3	2150 ± 340	12.0 ± 1.6	1.2 ± 0.2
Thr^{387} → Asn	1.0 ± 0.1	1.5 ± 0.2	$>5 \times 10^4$	0.7 ± 0.1	0.6 ± 0.2

[a]Reaction mixtures contained $(NH_4)_2Fe(SO_4)_2$ (10 μM), ascorbic acid (1 mM), 2OG (1−3000 μM), and CODD (10 μM) in 50 mM HEPES (pH 7.00) at 37 °C and the ambient O_2 concentration (217 μM). [b]Fluorescence titrations: PHD2 (1.1 μM), $MnSO_4$ (20 μM) in 50 mM HEPES (pH 7.00) titrated with 2OG (500 μM).

μM); the K_D was obtained by fitting the data to eq 2, in which the observed fluorescence intensity (I) is normalized to the intensity in the absence of 2OG (I_0) and the presence of a saturating 2OG concentration (I_f).

$$\frac{I - I_0}{I_f - I_0} = \Big[[\text{PHD2}] + [\text{2OG}] + K_D - \sqrt{([\text{PHD2}] + [\text{2OG}] + K_D)^2 - 4[\text{PHD2}][\text{2OG}]}\Big] / (2[\text{PHD2}]) \quad (2)$$

X-Band EPR of {FeNO}^{7}. Anaerobic samples were prepared in a glovebox (<1 ppm O_2) for analysis. $(NH_4)_2FeSO_4$ was brought into the glovebox as a solid and dissolved using degassed H_2O. The DEANO stocks were prepared in 10 mM NaOH in the glovebox, and the concentration was verified by its published extinction coefficient and characteristic UV absorbance at 250 nm.[19,20] A 100 μL EPR sample was prepared anaerobically and contained PHD2 (0.10 mM), $(NH_4)_2FeSO_4$ (0.10 mM), 2OG (0.50 mM), CODD (100 μM), and DEANO (0.5 mM) in 50 mM HEPES (pH 7.00) at room temperature (23 °C). The sample was aged for 20 min to allow the release of NO from DEANO and then flash-frozen in liquid nitrogen. EPR spectra were recorded using a Bruker Elexsys E-500 EPR instrument equipped with a DM4116 cavity and a Bruker ER 4118CF-O LHe/LN_2 cryostat at a frequency of 9.624 GHz, a power of 2.0 mW, a modulation amplitude of 10 G, a modulation frequency of 100 GHz, a time constant of 163 ms, and a temperature of 4 K. As the electronic structure of the $S = {}^3/_2$ ferrous-nitrosyl center is highly axial (E/D < 0.1), the observed EPR resonances (g_x, g_y, and g_z) were related to the rhombicity of the zero-field splitting (E/D) using an effective spin Hamiltonian (eq 3).[21]

$$g_x = g_0[2 - 3E/D - 3/2(E/D)^2] \quad (3a)$$

$$g_y = g_0[2 + 3E/D - 3/2(E/D)^2] \quad (3b)$$

$$g_z = g_0[1 - 3(E/D)^2] \quad (3c)$$

RESULTS AND DISCUSSION

Steady State Kinetics with Varied 2OG Concentrations. The structure of PHD2 showed a hydrogen bond network connecting 2OG, the aquo ligand, and Thr^{387} (Figure 1). As a hydrogen bonding residue is structurally conserved at this position in other 2OG oxygenases,[13,15] we hypothesized that this played an important role during turnover. To test the effect of this contact on steps between 2OG binding and ODD binding, initial rate data were measured as a function of varied 2OG concentration using saturating concentrations of Fe^{2+} (10 μM), CODD (10 μM), and ascorbate (1 mM); the O_2 concentration was fixed at ambient levels (217 μM). WT PHD2 exhibited simple saturation kinetics over the 2OG concentration range of 1−50 μM, with values of k_{cat} (2.3 min^{-1}) and $k_{cat}/K_{M(2OG)}$ (2.7 μM^{-1} min^{-1}) similar to those previously reported.[14,18,22−24] Similarly, the conservative Thr^{387} → Asn variant exhibited saturation kinetics over the tested concentration range, with rate constants modestly decreased relative to those of WT PHD2 (Table 1).

The initial rate data for the Thr^{387} → Ala variant were a significant contrast to those of WT PHD2. While Thr^{387} → Ala exhibited simple saturation kinetics for <250 μM 2OG, this variant exhibited ∼50% activity at 3000 μM 2OG (Figure 2).

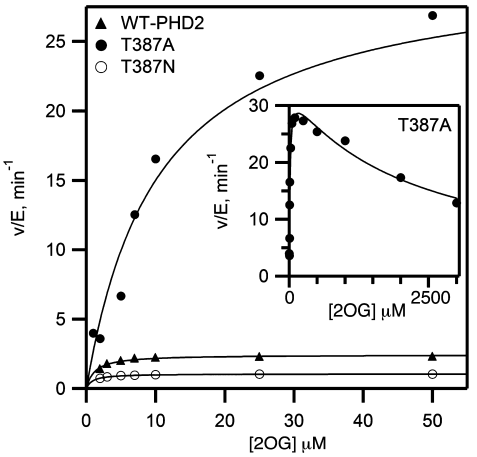

Figure 2. Steady state kinetics for PHD2 variants with varied 2OG concentrations. Reaction mixtures included $(NH_4)_2Fe(SO_4)_2$ (10 μM), ascorbic acid (1 mM), 2OG (1−3000 μM), and CODD (10 μM) in 50 mM HEPES (pH 7.00) at 37.0 °C and the ambient O_2 concentration (217 μM).

Fitting the initial rate data to a simple substrate inhibition model led to parameters k_{cat} (32.9 min^{-1}), $k_{cat}/K_{M(2OG)}$ (2.7 μM^{-1} min^{-1}), and $K_{I(2OG)}$ (2200 μM). The high value for k_{cat} indicated that Thr^{387} → Ala performed chemistry more rapidly than WT PHD2, but the observed substrate inhibition suggested that slow release of one of the products could limit turnover.

The steady state rate constant $k_{cat}/K_{M(2OG)}$ reflects those steps between 2OG binding and the subsequent irreversible step, which is CODD binding at saturating CODD concentrations. As this rate constant is essentially unchanged upon mutation of Thr^{387}, contacts from this residue do not affect these steps. In contrast, k_{cat} reflects nondiffusional steps and was greatly affected by mutation of Thr^{387}. While k_{cat} was unchanged in the conservative Thr^{387} → Asn variant, this kinetic parameter increased ∼15-fold for the Thr^{387} → Ala variant, suggesting that a chemical step was affected by the Thr^{387} variants.

DOI: 10.1021/bi501540c
Biochemistry 2015, 54, 2851−2857

The substrate inhibition observed for Thr^{387} → Ala prompted us to test the other variants for this effect. WT PHD2 retained >95% activity even at extremely high levels of 2OG; fits of these data to the substrate inhibition model were unsatisfactory [$K_{I(2OG)}$ > 26 mM], indicating that PHD2 did not undergo substrate inhibition. Thr^{387} → Asn similarly showed minimal inhibition at extremely high 2OG concentrations [$K_{I(2OG)}$ > 50 mM]. The absence of significant substrate inhibition observed for WT PHD2 was consistent with product release being rapid, consistent with the prior reports that implicated a step early in catalysis as being rate-limiting for WT PHD2.[10]

Substrate inhibition could arise from many possible mechanisms in which substrate binding leads to a lower-reactivity enzyme form. Inhibition by 2OG could be due to binding of 2OG to the Fe^{2+} cofactor in a geometry that prevented O_2 from reacting, or by binding to the Fe^{2+} when an equivalent of succinate or 2OG was already present. Although our kinetic data and 2OG binding data cannot distinguish among these possibilities, a unified model that accounts for the observed kinetics (see below) and substrate inhibition found for Thr^{387} → Ala is one in which chemistry is much faster than succinate release, such that the (Fe+Succ)PHD2 form of the enzyme accumulates in the steady state for this variant. Inhibition by 2OG or by CODD would arise from these substrates binding to the (Fe+Succ)PHD2 form of the enzyme, thereby preventing the enzyme from adopting the proper cofactor orientation to enter into catalysis.

The binding affinity for 2OG was measured for each of the variants by intrinsic tryptophan fluorescence quenching (Supporting Information). Binding curves were fit to a single-binding site model using eq 2, which indicated a similar avidity toward 2OG (K_D ~ 1 μM) for each variant. Attempts to fit a second 2OG binding event were not successful, possibly because of the large difference in magnitude between $K_{M(2OG)}$ and $K_{I(2OG)}$ for each of the variants.

Steady State Kinetics with Varied CODD Concentrations. The impact of Thr^{387} variants on the chemical steps of turnover was tested by measuring steady state kinetics with CODD as the varied substrate. Initial rates of CODD hydroxylation were measured as a function of varied CODD concentration in 50 mM HEPES (pH 7.00, 37.0 °C), with saturating concentrations of Fe^{2+} (10 μM), 2OG (100 μM), and ascorbate (1 mM); the O_2 concentration was fixed at the ambient level (217 μM). As O_2 was not saturating, $k_{cat}/K_{M(CODD)}$ will reflect steps from CODD binding to the irreversible chemistry involved with oxidative decarboxylation. Steady state kinetic constants, k_{cat} and $k_{cat}/K_{M(CODD)}$, were determined by fitting the data to the Michaelis–Menten equation (Figure 3). The rate constants for WT PHD2 were in good agreement with those of prior reports.[14,22,25] While the conservative Thr^{387} → Asn mutation led to rate constants that were modestly decreased compared to those of WT PHD2, those for the Thr^{387} → Ala variant were ~10-fold greater than those of WT PHD2, indicating that removal of the hydrogen bond from Thr^{387} greatly impacted chemical steps. The rate constants for Thr^{387} → Ala also exhibited pronounced substrate inhibition at elevated CODD concentrations (Figure 3).

The initial rate data for Thr^{387} → Ala were fit in two ways to adequately treat the inhibition. The first fit used the Michaelis–Menten equation to fit the initial rate data for CODD concentrations of <10 μM, leading to the following fitted parameters: k_{cat} = 33 min^{-1}, and $k_{cat}/K_{M(CODD)}$ = 13 μM^{-1} min^{-1}. These kinetic constants were remarkable because they suggested that the active site in WT PHD2 was arranged to slow turnover.

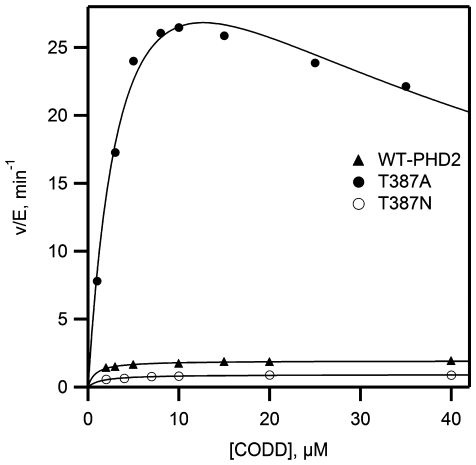

Figure 3. Steady state kinetic data with varied CODD concentrations. Reaction mixtures included $(NH_4)_2Fe(SO_4)_2$ (10 μM), ascorbic acid (1 mM), 2OG (100 μM), and CODD (2–40 μM) in 50 mM HEPES (pH 7.00) at 37.0 °C and the ambient O_2 concentration (217 μM).

The second fit used the substrate inhibition model and resulted in the following values: k_{cat} = 44 min^{-1}, $k_{cat}/K_{M(CODD)}$ = 11 μM^{-1} min^{-1}, and K_I = 38 μM (Table 2). This second fit reproduced the data well, suggesting that the peptide substrate (CODD) was a stronger inhibitor than 2OG toward the Thr^{387} → Ala variant. As for 2OG inhibition, inhibition by the CODD substrate could arise from many possible mechanisms in which CODD binding would lead to a low-activity enzyme form. A simple model that accounts for the kinetic changes for the Thr^{387} → Ala variant is one in which succinate release is slow, as this could lead to binding of either 2OG or CODD to the unreactive (Fe+succ)PHD2 enzyme form. The substrate inhibition by 2OG and CODD implicates a step after O_2 binding and/or activation as being rate-limiting in the Thr^{387} → Ala variant.

Table 2. Steady State Kinetic Constants, k_{cat} and $k_{cat}/K_{M(CODD)}$, with Varied CODD Concentrations[a]

enzyme	k_{cat} (min^{-1})	$k_{cat}/K_{M(CODD)}$ (μM^{-1} min^{-1})	K_I (μM)	K_M (μM)
WT PHD2	1.9 ± 0.1	2.4 ± 0.2	–	0.8 ± 0.1
Thr^{387} → Ala	44 ± 3	11 ± 1	38 ± 6	4.1 ± 0.7
Thr^{387} → Asn	0.9 ± 0.1	0.7 ± 0.1	–	1.4 ± 0.2

[a]Reaction mixtures contained $(NH_4)_2Fe(SO_4)_2$ (10 μM), ascorbic acid (1 mM), 2OG (100 μM), and CODD (2–50 μM) in 50 mM HEPES (pH 7.00) at 37.0 °C and the ambient O_2 concentration (217 μM).

Steady State Kinetics with Varied O_2 Concentrations. The increased rates of turnover for the Thr^{387} → Ala variant suggested that steps involved in O_2 activation were faster than for WT PHD2. The steady state kinetics as a function of varied O_2 concentration were measured to isolate steps between O_2 binding and oxidative decarboxylation (Table 3). The initial rate data showed simple saturation kinetics for all but the Thr^{387} → Ala variant and were fit to the Michaelis–Menten equation (Figure 4). Both WT PHD2 and the conservative

DOI: 10.1021/bi501540c
Biochemistry 2015, 54, 2851–2857

Table 3. Steady State Kinetic Parameters Using O_2 as the Varied Substrate[a]

enzyme	k_{cat} (min^{-1})	k_{cat}/K_M (μM^{-1} min^{-1})	K_M (μM)
WT PHD2	8 ± 0.7	0.015 ± 0.001	530 ± 90
Thr^{387} → Ala	29 ± 3	0.3 ± 0.1	100 ± 20
Thr^{387} → Asn	3.8 ± 0.5	0.005 ± 0.001	760 ± 170

[a]At 10 μM Fe^{2+}, 100 μM 2OG, 10 μM CODD, 37.0 °C, and pH 7.00.

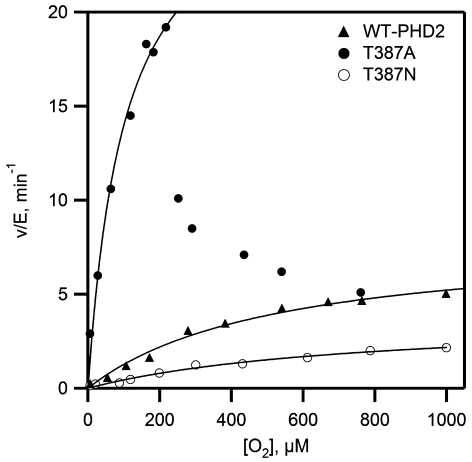

Figure 4. Steady state kinetics as a function of varied O_2 concentrations. Reaction mixtures included $(NH_4)_2Fe(SO_4)_2$ (10 μM), 2OG (100 μM), CODD (10 μM), and ascorbic acid (1 mM) in 50 mM HEPES (pH 7.00): (○) WT PHD2, (●) Thr^{387} → Asn, and (▲) Thr^{387} → Ala.

Thr^{387} → Asn variant exhibited sluggish reactivity toward O_2, with kinetic parameters for WT PHD2: $k_{cat}/K_{M(O2)}$ = 0.015 μM^{-1} min^{-1} (~0.25 × 10^{-9} M^{-1} s^{-1}), and $K_{M(O_2)}$ = 530 μM, consistent with prior reports.[28,29] The high $K_{M(O_2)}$ has been rationalized as being necessary for hypoxia sensing, as PHD2 activity would be proportionate to physiologically relevant levels of O_2.[30] The Thr^{387} → Ala variant is a contrast to this, as $k_{cat}/K_{M(O_2)}$ = 0.3 μM^{-1} min^{-1}, a 20-fold increase in reaction rate versus that of WT PHD2, which indicates that steps involving O_2 activation have markedly increased the rate for this variant. The Thr^{387} → Ala variant also exhibited saturation kinetics up to 220 μM O_2, but with an activity that was only ~25% of maximal at elevated O_2 concentrations (Figure 4). Attempts to fit this activity curve to a variety of inhibition models led to unsatisfactory fits, suggesting that the decreased activity at high O_2 concentrations may reflect enzyme inactivation, which is seen for several other 2OG oxygenases.[31−34]

As our experimental conditions used saturating levels of 2OG and CODD, the macroscopic rate constant $[k_{cat}/K_{M(O_2)}]$ reports only on steps between O_2 binding and the subsequent irreversible step, which in the consensus mechanism for PHD2 is oxidative decarboxylation. The increased values for k_{cat} and $k_{cat}/K_{M(O_2)}$ observed for Thr^{387} → Ala point definitively to an increased rate for oxidative decarboxylation in this variant versus that observed for WT PHD2.

The kinetic parameters for the Thr^{387} → Ala variant are remarkable for two reasons. First, the increased $k_{cat}/K_{M(O_2)}$ and related mechanistic data indicate that chemistry has become faster as a result of this point mutation, underscoring the enormous influence over oxidative decarboxylation exerted by second-sphere contacts in PHD2. This implies that O_2 activation is not just a function of the redox potential at the Fe^{2+} cofactor but will include the polar environment near the 2OG and the distal O atom of bound O_2. Second, the Thr^{387} → Ala variant has a $K_{M(O_2)}$ lower than that found for WT PHD2, making for a more sensitive activity response to changes in O_2 concentration, particularly over the physiological O_2 range of <50 μM. This opens the possibility of using enzyme delivery[35] or engineering approaches to tailor the hypoxia response within cells.

EPR Spectra of (Fe^{2+}NO)PHD2. According to the consensus mechanism, PHD2 must bind O_2 such that the distal O atom can attack the 2-oxo position of 2OG. We propose that Thr^{387} of WT PHD2 favors a specific gas binding geometry such that the bound O_2 is not positioned optimally for reaction with 2OG. As NO binds to Fe^{2+} in non-heme enzymes to form a spectroscopically accessible $S = {}^3/_2$ {FeNO}^{7} and adopts a bent geometry similar to that of bound O_2,[26,27,36,37] we used EPR line shape analysis to assess the impact of Thr^{387} on bound gas geometry.

The EPR line shape of {FeNO}^{7} centers in 2OG oxygenases and related enzymes is dominated by the large zero-field splitting,[36−38] with EPR features near g_{eff} ~ 2 and g_{eff} ~ 4 that are sensitive reporters of the rhombic zero-field splitting parameter (E/D).[21] Rhombic zero-field splitting can be directly calculated by use of eq 3, relating the observed g_{eff} values to the E/D ratio. As the zero-field splitting arises from admixture of the low-lying excited states into the ground state, the E/D ratio ultimately reports on the geometry of the {FeNO}^{7} spin center. For example, the EPR line shape of the {FeNO}^{7} center is very sensitive to the Fe−N−O bond angle in sterically constrained model complexes[39] as well as equatorial bonding in non-heme proteins[21,37] because of the splitting of the g_{eff} ~ 4 features caused by rhombic zero-field splitting.

Ferrous nitrosyl complexes of WT PHD2 and the Thr^{387} → Ala variant were prepared by anaerobically generating NO in the presence of the (Fe+2OG)PHD2/CODD form of each enzyme. The X-band EPR spectra were recorded at 4 K in a liquid helium flow cryostat, showing a complex line shape near g_{eff} = 4 for both samples (Figure 5). The {FeNO}^{7} center of WT PHD2 exhibited intense features at g_{eff} = 4.08 and 3.96,

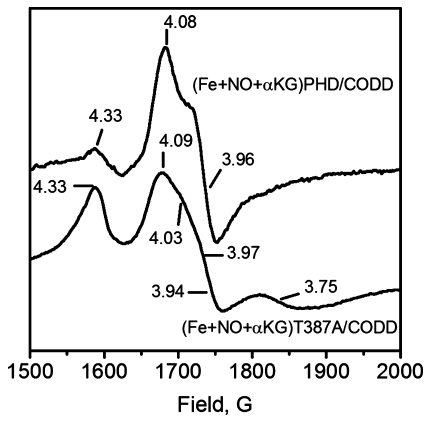

Figure 5. X-Band EPR of (Fe^{2+}+NO+2OG)PHD2/CODD. PHD2 (100 μM), CODD (100 μM), $(NH_4)_2FeSO_4$ (100 μM), 2OG (500 μM), and DEANO (500 μM) in 50 mM HEPES (pH 7.00), with a frequency of 9.624 GHz, a power of 2.0 mW, a modulation amplitude of 10 G, a modulation of 100 GHz, and a temperature of 4 K.

DOI: 10.1021/bi501540c
Biochemistry 2015, 54, 2851−2857

which arose from an $S = {}^3/_2$ spin with a highly axial zero-field splitting ($E/D = 0.011$), as well as a minor feature at $g_{eff} \sim 4.3$ that likely arose from adventitious Fe^{3+}. In contrast, the $\{FeNO\}^7$ center of $Thr^{387} \rightarrow Ala$ was more complex, with two $S = {}^3/_2$ species evident. One species was very similar to that observed for WT PHD2, with $g_{eff} = 4.09$ and 3.94 ($E/D = 0.014$); the second center was much more rhombic, with $g_{eff} = 4.33$ and 3.75 ($E/D = 0.48$).

Although it is not possible to ascribe specific geometries to each of these spin centers, the $Thr^{387} \rightarrow Ala$ mutation led to an $\{FeNO\}^7$ center much more heterogeneous than that found in WT PHD2. This likely arose from the steric interactions between the bound NO and contacts with the active site environment. Coupled with the observed increase in activity for $Thr^{387} \rightarrow Ala$, this suggests that the geometry of bound gas is correlated with O_2 activation such that WT PHD2 positions the bound gas in a nonoptimal orientation for oxidative decarboxylation. In the consensus mechanism, O_2 binds as a putative ($Fe^{3+}O_2^{-}$) adduct, which then attacks the C-2 keto position of 2OG to initiate oxidative decarboxylation. Should the distal O atom be stabilized by an electric dipole interaction with the hydroxyl group of Thr^{387}, it could be less nucleophilic in WT PHD2. Alternately, Thr^{387} could cause the distal O atom to be oriented away from the C-2 keto position, thereby lowering the reactivity of the putative superoxide in WT PHD2.

Implications for Hypoxia Sensing. Why is turnover so slow for WT PHD2, and how could removing the hydrogen bonds from Thr^{387} increase the kinetic parameters for O_2 activation? The answers to both of these questions are speculative at this point, but considering the structural and mechanistic data for PHD2 within the context of the physiological role of this enzyme points to the intriguing possibility that the naturally occurring residue is part of the machinery that limits maximal turnover.

As the physiological role of PHD2 is to turn off gene expression, it is very likely that this enzyme fulfills its role while turning over on a time scale of minutes; this lack of evolutionary pressure to increase reaction rates may lead to an active site optimized for something other than rapid turnover. Single-turnover experiments indicated that the hydroxylated CODD product formed on a time scale of minutes ($k_{obs} = 0.018\ s^{-1}$, 5 °C) without any accumulating intermediates.[10] As this rate constant is virtually identical to that observed in the steady state ($k_{cat} = 0.03\ s^{-1}$, 37 °C),[14] it is very likely that oxidative decarboxylation is rate-limiting in WT PHD2. This is unusual for 2OG-dependent oxygenases but may reflect the O_2 sensing function of PHD2.

The implications of this work are 2-fold. First, contacts within the active site control the O_2 activation rate in 2OG oxygenases. Second, PHD2 can be engineered into a form more active than that found in nature, in particular with respect to the reactivity at low O_2 concentrations. Although this was achieved by point mutagenesis in this report, one can envision the use of small molecules to target the distal hydrogen bonding in PHD2. Achieving an increased rate of turnover under hypoxic conditions would lead to altered cellular hypoxia sensing.

■ ASSOCIATED CONTENT

Supporting Information

Experimental measurement of $K_{D(2OG)}$ for PHD2 variants. The Supporting Information is available free of charge on the ACS Publications website at DOI: 10.1021/bi501540c.

■ AUTHOR INFORMATION

Corresponding Author

*E-mail: mknapp@chem.umass.edu. Phone: (413) 545-4001. Fax: (413) 545-4490.

Funding

This research was supported by the National Institutes of Health (NIH) (Grant 1R01-GM077413 to M.J.K.), NIH Chemistry-Biology Interface Predoctoral Training Grant T32-GM008515 to C.Y.T., and the Turkish Ministry of National Education (S.P.).

Notes

The authors declare no competing financial interest.

■ ABBREVIATIONS

2OG, 2-oxoglutarate or α-ketoglutarate; AtsK, alkylsulfatase; FIH, factor-inhibiting HIF; HAT, hydrogen atom transfer; HEPES, 4-(2-hydroxyethyl)-1-piperazineethanesulfonic acid; HIF, hypoxia-inducible factor-1α; MALDI-TOF-MS, matrix-assisted laser desorption ionization time-of-flight mass spectrometry; PHD2, prolyl hydroxylase domain 2; TauD, taurine dioxygenase.

■ REFERENCES

(1) Berra, E., Benizri, E., Ginouvès, A., Volmat, V., Roux, D., and Pouysségur, J. (2003) HIF prolyl-hydroxylase 2 is the key oxygen sensor setting low steady-state levels of HIF-1α in normoxia. *EMBO J. 22*, 4082−4090.

(2) Appelhoff, R. J., Tian, Y.-M., Raval, R. R., Turley, H., Harris, A. L., Pugh, C. W., Ratcliffe, P. J., and Gleadle, J. M. (2004) Differential function of the prolyl hydroxylases PHD1, PHD2, and PHD3 in the regulation of hypoxia-inducible factor. *J. Biol. Chem. 279*, 38458−38465.

(3) Bruick, R. K. (2003) Oxygen sensing in the hypoxic response pathway: Regulation of the hypoxia-inducible transcription factor. *Genes Dev. 17*, 2614−2623.

(4) Jaakkola, P., Mole, D. R., Tian, Y. M., Wilson, M. I., Gielbert, J., Gaskell, S. J., Kriegsheim, Av., Hebestreit, H. F., Mukherji, M., Schofield, C. J., Maxwell, P. H., Pugh, C. W., and Ratcliffe, P. J. (2001) Targeting of HIF-α to the von Hippel-Lindau ubiquitylation complex by O_2-regulated prolyl hydroxylation. *Science 292*, 468−472.

(5) Aprelikova, O., Chandramouli, G. V. R., Wood, M., Vasselli, J. R., Riss, J., Maranchie, J. K., Linehan, W. M., and Barrett, J. C. (2004) Regulation of HIF prolyl hydroxylases by hypoxia-inducible factors. *J. Cell. Biochem. 92*, 491−501.

(6) Hewitson, K. S., and Schofield, C. J. (2004) The HIF pathway as a therapeutic target. *Drug Discovery Today 9*, 704−711.

(7) Speer, R. E., Karuppagounder, S. S., Basso, M., Sleiman, S. F., Kumar, A., Brand, D., Smirnova, N., Gazaryan, I., Khim, S. J., and Ratan, R. R. (2013) Hypoxia-inducible factor prolyl hydroxylases as targets for neuroprotection by "antioxidant" metal chelators: From ferroptosis to stroke. *Free Radical Biol. Med. 62*, 26−36.

(8) Hoffart, L. M., Barr, E. W., Guyer, R. B., Bollinger, J. M., and Krebs, C. (2006) Direct spectroscopic detection of a C-H-cleaving high-spin Fe(IV) complex in a prolyl-4-hydroxylase. *Proc. Natl. Acad. Sci. U.S.A. 103*, 14738−14743.

(9) Krebs, C., Galonić Fujimori, D., Walsh, C. T., and Bollinger, J. M. (2007) Non-heme Fe(IV)-oxo intermediates. *Acc. Chem. Res. 40*, 484−492.

(10) Flashman, E., Hoffart, L. M., Hamed, R. B., Bollinger, J. M., Krebs, C., and Schofield, C. J. (2010) Evidence for the slow reaction of hypoxia-inducible factor prolyl hydroxylase 2 with oxygen. *FEBS J. 277*, 4089−4099.

(11) Price, J. C., Barr, E. W., Tirupati, B., Bollinger, J. M., and Krebs, C. (2003) The first direct characterization of a high-valent iron intermediate in the reaction of an α-ketoglutarate-dependent dioxygenase: A high-spin Fe^{IV} complex in taurine/α-ketoglutarate

DOI: 10.1021/bi501540c
Biochemistry 2015, 54, 2851−2857

dioxygenase (TauD) from *Escherichia coli*. *Biochemistry 42*, 7497−7508.
(12) Grzyska, P. K., Ryle, M. J., Monterosso, G. R., Liu, J., Ballou, D. P., and Hausinger, R. P. (2005) Steady-state and transient kinetic analyses of taurine/α-ketoglutarate dioxygenase: Effects of oxygen concentration, alternative sulfonates, and active-site variants on the FeIV-oxo intermediate. *Biochemistry 44*, 3845−3855.
(13) Hangasky, J. A., Saban, E., and Knapp, M. J. (2013) Inverse Solvent Isotope Effects Arising from Substrate Triggering in the Factor Inhibiting Hypoxia Inducible Factor. *Biochemistry 52*, 1594−1602.
(14) Flagg, S. C., Giri, N., Pektas, S., Maroney, M. J., and Knapp, M. J. (2012) Inverse solvent isotope effects demonstrate slow aquo release from hypoxia inducible factor-prolyl hydroxylase (PHD2). *Biochemistry 51*, 6654−6666.
(15) Hangasky, J. A., Taabazuing, C. Y., Valliere, M. A., and Knapp, M. J. (2013) Imposing function down a (cupin)-barrel: Secondary structure and metal stereochemistry in the αKG-dependent oxygenases. *Metallomics 5*, 287−301.
(16) Rosen, M. D., Venkatesan, H., Peltier, H. M., Bembenek, S. D., Kanelakis, K. C., Zhao, L. X., Leonard, B. E., Hocutt, F. M., Wu, X., Palomino, H. L., Brondstetter, T. I., Haugh, P. V., Cagnon, L., Yan, W., Liotta, L. A., Young, A., Mirzadegan, T., Shankley, N. P., Barrett, T. D., and Rabinowitz, M. H. (2010) Benzimidazole-2-pyrazole HIF Prolyl 4-Hydroxylase Inhibitors as Oral Erythropoietin Secretagogues. *ACS Med. Chem. Lett. 1*, 526−529.
(17) Cascella, B., and Mirica, L. M. (2012) Kinetic analysis of iron-dependent histone demethylases: α-Ketoglutarate substrate inhibition and potential relevance to the regulation of histone demethylation in cancer cells. *Biochemistry 51*, 8699−8701.
(18) Pektas, S., and Knapp, M. J. (2013) Substrate preference of the HIF-prolyl hydroxylase-2 (PHD2) and substrate-induced conformational change. *J. Inorg. Biochem. 126*, 55−60.
(19) Maragos, C. M., Morley, D., Wink, D. A., Dunams, T. M., Saavedra, J. E., Hoffman, A., Bove, A. A., Isaac, L., Hrabie, J. A., and Keefer, L. K. (1991) Complexes of NO with Nucleophiles as Agents for the Controlled Biological Release of Nitric Oxide. Vasorelaxant Effects. *J. Med. Chem. 34*, 3242−3247.
(20) Keefer, L. K., Nims, R. W., Davies, K. M., and Wink, D. A. (1996) "NONOates" (1-Substituted Diazen-1-ium-1,2-diolates) as Nitric Oxide Donors: Convenient Nitric Oxide Dosage Forms. *Methods Enzymol. 268*, 281−293.
(21) Arcierog, D. M., Orville, A. M., and Lipscomb, J. D. (1985) [^{17}O]Water and Nitric Oxide Binding by Protocatechuate 4,5-Dioxygenase and Catechol 2,3-Dioxygenase. *J. Biol. Chem. 260*, 14035−14044.
(22) Flagg, S. C., Martin, C. B., Taabazuing, C. Y., Holmes, B. E., and Knapp, M. J. (2012) Screening chelating inhibitors of HIF-prolyl hydroxylase domain 2 (PHD2) and factor inhibiting HIF (FIH). *J. Inorg. Biochem. 113*, 25−30.
(23) Chowdhury, R., McDonough, M. A., Mecinović, J., Loenarz, C., Flashman, E., Hewitson, K. S., Domene, C., and Schofield, C. J. (2009) Structural basis for binding of hypoxia-inducible factor to the oxygen-sensing prolyl hydroxylases. *Structure 17*, 981−989.
(24) Koivunen, P., Hirsilä, M., Kivirikko, K. I., and Myllyharju, J. (2006) The length of peptide substrates has a marked effect on hydroxylation by the hypoxia-inducible factor prolyl 4-hydroxylases. *J. Biol. Chem. 281*, 28712−28720.
(25) Flashman, E., Bagg, E. A. L., Chowdhury, R., Mecinović, J., Loenarz, C., McDonough, M. A., Hewitson, K. S., and Schofield, C. J. (2008) Kinetic rationale for selectivity toward N- and C-terminal oxygen-dependent degradation domain substrates mediated by a loop region of hypoxia-inducible factor prolyl hydroxylases. *J. Biol. Chem. 283*, 3808−3815.
(26) Brown, C. A., Pavlosky, M. A., Westre, T. E., Zhang, Y., Hedman, B., Hodgson, K. O., and Solomon, E. I. (1995) Spectroscopic and Theoretical Description of the Electronic Structure of S = 3/2 Iron-Nitrosyl Complexes and Their Relation to O_2 Activation by Non-Heme Iron Enzyme Active Sites. *J. Am. Chem. Soc. 117*, 715−732.
(27) Muthukumaran, R. B., Grzyska, P. K., Hausinger, R. P., and McCracken, J. (2007) Probing the iron-substrate orientation for taurine/α-ketoglutarate dioxygenase using deuterium electron spin echo envelope modulation spectroscopy. *Biochemistry 46*, 5951−5959.
(28) Ehrismann, D., Flashman, E., Genn, D. N., Mathioudakis, N., Hewitson, K. S., Ratcliffe, P. J., and Schofield, C. J. (2007) Studies on the activity of the hypoxia-inducible-factor hydroxylases using an oxygen consumption assay. *Biochem. J. 401*, 227−234.
(29) Hirsilä, M., Koivunen, P., Günzler, V., Kivirikko, K. I., and Myllyharju, J. (2003) Characterization of the human prolyl 4-hydroxylases that modify the hypoxia-inducible factor. *J. Biol. Chem. 278*, 30772−30780.
(30) Aragonés, J., Schneider, M., Van Geyte, K., Fraisl, P., Dresselaers, T., Mazzone, M., Dirkx, R., Zacchigna, S., Lemieux, H., Jeoung, N. H., Lambrechts, D., Bishop, T., Lafuste, P., Diez-Juan, A., Harten, S. K., Van Noten, P., De Bock, K., Willam, C., Tjwa, M., Grosfeld, A., Navet, R., Moons, L., Vandendriessche, T., Deroose, C., Wijeyekoon, B., Nuyts, J., Jordan, B., Silasi-Mansat, R., Lupu, F., Dewerchin, M., Pugh, C., Salmon, P., Mortelmans, L., Gallez, B., Gorus, F., Buyse, J., Sluse, F., Harris, R. A., Gnaiger, E., Hespel, P., Van Hecke, P., Schuit, F., Van Veldhoven, P., Ratcliffe, P., Baes, M., Maxwell, P., and Carmeliet, P. (2008) Deficiency or inhibition of oxygen sensor Phd1 induces hypoxia tolerance by reprogramming basal metabolism. *Nat. Genet. 40*, 170−180.
(31) Chen, Y.-H., Comeaux, L. M., Eyles, S. J., and Knapp, M. J. (2008) Auto-hydroxylation of FIH-1: An Fe(II), α-ketoglutarate-dependent human hypoxia sensor. *Chem. Commun.*, 4768−4770.
(32) Ryle, M. J., Koehntop, K. D., Liu, A., Que, L., and Hausinger, R. P. (2003) Interconversion of two oxidized forms of taurine/α-ketoglutarate dioxygenase, a non-heme iron hydroxylase: Evidence for bicarbonate binding. *Proc. Natl. Acad. Sci. U.S.A. 100*, 3790−3795.
(33) Mantri, M., Zhang, Z., McDonough, M. A., and Schofield, C. J. (2012) Autocatalysed oxidative modifications to 2-oxoglutarate dependent oxygenases. *FEBS J. 279*, 1563−1575.
(34) Liu, A., Ho, R. Y., Que, L., Ryle, M. J., Phinney, B. S., and Hausinger, R. P. (2001) Alternative reactivity of an α-ketoglutarate-dependent iron(II) oxygenase: Enzyme self-hydroxylation. *J. Am. Chem. Soc. 123*, 5126−5127.
(35) Fu, A., Tang, R., Hardie, J., Farkas, M. E., and Rotello, V. M. (2014) Promises and pitfalls of intracellular delivery of proteins. *Bioconjugate Chem. 25*, 1602−1608.
(36) Ye, S., Price, J. C., Barr, E. W., Green, M. T., Bollinger, J. M., Pennsyl, V., Uni, S., and Park, U. V. (2010) Cryoreduction of the NO-Adduct of Taurine: α-Ketoglutarate Dioxygenase (TauD) Yields an Elusive {FeNO}^{8} Species. *J. Am. Chem. Soc. 132*, 4739−4751.
(37) Han, A. Y., Lee, A. Q., and Abu-Omar, M. M. (2006) EPR and UV-vis studies of the nitric oxide adducts of bacterial phenylalanine hydroxylase: Effects of cofactor and substrate on the iron environment. *Inorg. Chem. 45*, 4277−4283.
(38) Hausinger, R. P. (2004) Fe^{II}/α-ketoglutarate-dependent hydroxylases and related enzymes. *Crit. Rev. Biochem. Mol. Biol. 39*, 21−68.
(39) Ray, M., Golombek, A. P., Hendrich, M. P., Yap, G. P. A., Liable-Sands, L. M., Rheingold, A. L., and Borovik, A. S. (1999) Structure and Magnetic Properties of Trigonal Bipyramidal Iron Nitrosyl Complexes. *Inorg. Chem. 38*, 3110−3115.

DOI: 10.1021/bi501540c
Biochemistry 2015, 54, 2851−2857